Phase diagram and optical conductivity of the one-dimensional spinless Holstein model

Q. Wang* and H. Zheng

*Department of Applied Physics, Shanghai Jiao Tong University, Shanghai 200030, People's Republic of China
and Physics Department, Xinjiang Normal University, Uromuq 830053, People's Republic of China*

M. Avignon

*Laboratoire d'Etudes des Proprietes Electroniques des Solides, Centre National de la Recherche Scientifique, Boîte Postale 166,
38042 Grenoble Cedex 9, France*

The effects of quantum lattice fluctuations on the Peierls transition and the optical conductivity in the one-dimensional Holstein model of spinless fermions have been studied by developing an analytical approach based on the unitary transformation method. We show that when the electron-phonon coupling constant decreases to a finite critical value, the Peierls dimerization is destroyed by the quantum lattice fluctuations. The dimerization gap is much more reduced by the quantum lattice fluctuations than the phonon order parameter. The calculated optical conductivity does not have the inverse-square-root singularity, but it has a peak above the gap edge, and there exists a significant tail below the peak. The peak of optical-conductivity spectrum is not directly corresponding to the dimerized gap. Our results of the phase diagram and the spectral-weight function agree with those of the density-matrix renormalization group and the exact diagonalization methods.

A great deal of quasi-one-dimensional materials, for example, the halogen-bridged mixed-valence transition-metal complexes, the conducting polymers, and the organic and inorganic spin-Peierls systems, exhibit an instability against a periodic lattice distortion due to the Peierls dynamics. Among the models for one-dimensional systems, the Holstein Hamiltonian[1] is a typical electron-phonon coupling model studied by many previous authors. An interesting and still controversial problem is how the dimerized ground state is modified when quantum lattice fluctuations are taken into account. The quantum lattice fluctuations could have an important effect in most quasi-one-dimensional materials with a dimerized ground state because the lattice zero-point motion is often comparable to the amplitude of the Peierls distortion.[2] The challenge of understanding the physics of quantum lattice fluctuations has led to an intense study of the Holstein model. Generally speaking, the nonadiabatic effect suppresses the order parameters of the system.[3] As far as the optical absorption is concerned, the results of adiabatic approximations have inverse-square-root singularity at the gap edge. However, this approach is questionable, and it has been shown that the quantum lattice fluctuations must be taken into account to satisfactorily describe some physical properties of quasi-one-dimensional systems.[4] By considering the nonadiabatic effect, the singularity may disappear.[5] The influences of the phonon frequency on the optical-conductivity spectrum in the range from $\omega_0 = 0$ to $\omega_0 \to \infty$ should be studied for understanding the physics of electron-phonon interactions in the nonadiabatic case.

When the quantum lattice fluctuations are taken into account, the theoretical analysis becomes much more difficult. In the past several years, the Holstein Hamiltonian has been investigated using various numerical approaches, such as Green's-function Monte Carlo simulation,[6,7] renormalization-group analysis,[8,9] variational method of the squeezed-polaron wave function,[10] phenomenological approach,[2] exact diagonalization,[11] etc. Very recently, works using numerical approaches have been performed in relation to the Peierls transition and the optical conductivity in the one-dimensional Holstein model of spinless fermions by using the density-matrix renormalization-group[12] and exact-diagonalization[13] methods. However, as was pointed out in Ref. 13, because of the effects of limited system sizes in numerical approaches, the precise determination of the critical value in the small ω_0 regime is somewhat difficult, and the precise extraction of the dimerized gap from optical-conductivity data is prevented. An analytical study of the Holstein model will make it possible to have an insight into the intrinsic properties of the molecular crystal materials. In a recent work, two of us[14] studied this model and investigated the dimerization order parameters and density of states in the gapped phase, and the velocity of charge excitations and the Luttinger liquid stiffness constant in the gapless phase. In this paper, we concentrate on the properties of the phase transition and the optical responses of the system with the view of understanding the effects of quantum lattice fluctuations on the Peierls instability and the optical conductivity in the Holstein model. We will show that our results of the phase diagram and the spectral-weight function agree surprisingly well with those of the density-matrix renormalization-group[12] and the exact-diagonalization[13] methods, and in our theory, the critical value can be determined precisely even for extremely small phonon frequency. The effects of quantum lattice fluctuations on the dimerized gap and on the order parameters are essentially different. The peak of optical-conductivity spectrum is not directly corresponding to the dimerization gap.

The one-dimensional spinless Holstein model in momentum space is

$$H = \sum_q \omega_0 b_q^\dagger b_q + \sum_k \epsilon_k c_k^\dagger c_k - \frac{1}{\sqrt{N}} \sum_{q,k} g(b_q + b_{-q}^\dagger) c_{k+q}^\dagger c_k,$$

$$(1)$$

where $\epsilon_k = -2t \cos k$ is the bare band structure, t the hopping integral, and N the total number of sites. c_k and b_q are the annihilation operators of electrons with momentum k and phonons with momentum q, respectively. The dispersionless phonon frequency $\omega_0 = \sqrt{K/M}$ and g is the electron-phonon coupling, K the elastic constant, and M the mass of ions (throughout this paper, we set $\hbar = k_B = 1$).

In order to take into account the electron-phonon correlation, the unitary transformation approach is used to treat H,[14] $\tilde{H} = e^S H e^{-S}$. After averaging the transformed Hamiltonian over the phonon vacuum state, we get an effective Hamiltonian for the fermions

$$H_{\text{eff}} = \frac{1}{2} K N u_0^2 + \sum_k E_0(k) c_k^\dagger c_k - \sum_{k>0} \Delta_0(k)(c_{k-\pi}^\dagger c_k$$

$$+ c_k^\dagger c_{k-\pi}) - \frac{1}{N} \sum_{q,k,k'} \frac{g^2}{\omega_0} \delta(k+q,k)$$

$$\times [2 - \delta(k'-q,k')] c_{k+q}^\dagger c_k c_{k'-q}^\dagger c_{k'},$$

$$(2)$$

where

$$E_0(k) = \epsilon_k - \frac{1}{N} \sum_{k'} \frac{g^2}{\omega_0^2} \delta(k',k) \delta(k,k')(\epsilon_k - \epsilon_{k'}), \quad (3)$$

$$\Delta_0(k) = \alpha u_0 [1 - \delta(k - \pi, k)], \quad (4)$$

$\alpha = g\sqrt{2M\omega_0}$, and $\delta(k+q,k) = 1/(1 + |\epsilon_{k+q} - \epsilon_k|/\omega_0)$ is a function of the energies of the incoming and outgoing fermions in the electron-phonon scattering process. This effective Hamiltonian works well in the $\omega_0 = 0$ and $\omega_0 \to \infty$ limits.

u_0 can be determined by the variational principle,

$$u_0 = \frac{\alpha}{KN} \sum_{k>0} [1 - \delta(k-\pi,k)] \langle fe|(c_{k-\pi}^\dagger c_k + c_k^\dagger c_{k-\pi})|fe\rangle.$$

$$(5)$$

Here, $|fe\rangle$ is the ground state of H_{eff}. Thus, the total Hamiltonian can be written as $\tilde{H} = \tilde{H}_0 + \tilde{H}_1$, where $\tilde{H}_1$ includes the terms that are zero after being averaged over the phonon vacuum state and

$$\tilde{H}_0 = \sum_q \omega_0 b_q^\dagger b_q + H_{\text{eff}}. \quad (6)$$

By means of the Green's-function method to implement the perturbation treatment on the four-fermion term in Eq. (2), we get the renormalized band function and the gap function[14]

$$E_k = E_0(k) - \frac{2t\lambda}{N} \sum_{k'>0} \{\delta(k',k)[2 - \delta(k',k)] - \delta(k'-\pi,k)$$

$$\times [2 - \delta(k'-\pi,k)]\} \frac{E_0(k')}{\sqrt{E_0^2(k') + \Delta_0^2(k')}}, \quad (7)$$

$$\Delta_k = \alpha u_0 [c - d\,\delta(k-\pi,k)], \quad (8)$$

where the dimensionless coupling $\lambda = g^2/2t\omega_0$, $W_k = \sqrt{E_k^2 + \Delta_k^2}$ is the fermionic spectrum in the gapped state, and

$$c = 1 + \frac{2t\lambda}{N} \sum_{k>0} [\delta(k-\pi,k) - V] \frac{\Delta_0(k)}{\alpha u_0 \sqrt{E_0^2(k) + \Delta_0^2(k)}}, \quad (9)$$

$$d = 1 - \frac{2t\lambda}{N} \sum_{k>0} [1 - \delta(k-\pi,k)] \frac{\Delta_0(k)}{\alpha u_0 \sqrt{E_0^2(k) + \Delta_0^2(k)}}, \quad (10)$$

$$V = \frac{1}{N^3} \sum_{q,k,k'} \delta(k,k+q)[2 - \delta(k',k'-q)] \quad (11)$$

is the on-site interaction that should be subtracted because of the Pauli principle.

The phonon-staggered ordering parameter is

$$m_p = \frac{1}{N} \sum_l (-1)^l \langle u_l \rangle = \frac{\alpha}{KN} \sum_{k>0} \frac{\Delta(k)}{W(k)}. \quad (12)$$

These are basic equations in our theory.

From Eq. (5), with $u_0 = 0$, we get the self-consistent equation of phase-transition points in the $g^2/\omega_0 \sim \omega_0$ plane,

$$1 = \frac{4t\lambda}{N} \sum_{k>0} [1 - \delta(k-\pi,k)] \frac{c - d\,\delta(k-\pi,k)}{|E_k|}. \quad (13)$$

If $\omega_0 = 0$, we have $\delta(k',k) = 0$ and $c = 1$, and Eq. (5) becomes the same as that in the adiabatic theory. In our theory, $\delta(k-\pi,k)$ has a sharp peak at the Fermi point and since $1 - \delta(k-\pi,k) = 4t|\cos k|/(\omega_0 + 4t|\cos k|)$, the logarithmic singularity in the integration of Eq. (5) in the adiabatic case is removed as long as the ratio ω_0/t_0 is finite. Comparing Eq. (8) with that in the adiabatic case, $\Delta = \alpha u_0$, we have the gap in the nonadiabatic case,

$$\Delta = \Delta(\pi/2) = \alpha u_0 [c - d]. \quad (14)$$

This is the true gap in the fermionic spectrum.

Figure 1 shows the ground-state phase diagram in the $g/\omega_0 \sim t/\omega_0$ plane. The solid line is our analytical result. For comparison, the results of previous authors are also shown. The line with circles and the line with squares denote the results of the density-matrix renormalization group (DMRG)[12] and the two-cutoff renormalization group (TCRG),[15] respectively. The line with triangles is the phase boundary of the variational Lanczos approach based on the inhomogeneous modified variational Lang-Firsov transformation (IMVLF).[13] To check the consistency of the phase
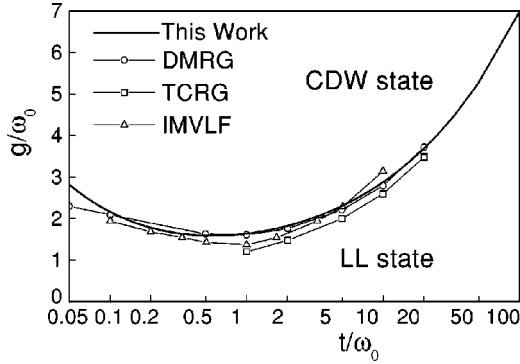
FIG. 1. The ground-state phase diagram in the $g/\omega_0 \sim t/\omega_0$ plane. The solid line is our analytical result. The line with open circles and the line with open squares denote the results of the density-matrix renormalization-group (DMRG) and the two-cutoff renormalization-group (TCRG) methods, respectively. The line with open triangles is the phase boundary of the variational Lanczos approach (IMVLF).

transition quantitatively with that of DMRG, some critical values g_c are listed in Table I. One can see from both the figure and the table that our results agree surprisingly well with that of DMRG except for very large ω_0 ($\omega_0/t \gtrsim 10$). Furthermore, our theory can get the phase boundary, separating Luttinger liquid and insulation [charge density wave (CDW)] phases, even in the very small ω_0 regime, which is theoretically and experimentally significant since, from the view point of experiment, for quite a lot of realistic cases, the frequency of the quantum phonon ω_0 is small. It seems that in the DMRG and the finite-lattice Lanczos approach, because of the effects of limited system sizes, the precise determination of the critical value in the small ω_0 regime is somewhat difficult.[13] The infinite system is never really gapless within the adiabatic approach, because the gap remains nonzero, although it becomes very small for weak electron-phonon coupling. On the contrary, in our theory, the logarithmic singularity $\int_0^{\pi/2} dk/\cos k$ in the integration of Eq. (5) is removed by the factor $1 - \delta(k - \pi, k)$, and the critical value λ_c can be determined precisely even for extremely small phonon frequency.

Inspired by the success of obtaining the phase diagram, we further investigate the dimerization gap and the optical responses.

Figure 2 shows the dimerization gap $\Delta/t = \Delta(\pi/2)/t$ and the phonon order parameter $\alpha m_p/t$ as functions of the phonon frequency ω_0/t for $\lambda = 0.81$. It is most notable that there is a discontinuous drop in the dimerization gap once the phonon frequency changes, no matter how small it is, from zero to finite, though at the adiabatic limit the dimerization
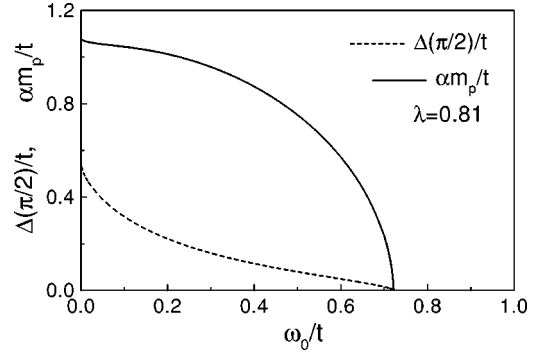

FIG. 2. The dimerization gap $\Delta/t = \Delta(\pi/2)/t$ and the order parameter $\alpha m_p/t$ as functions of the phonon frequency ω_0/t in the case of $\lambda = 0.81$.

gap is $\Delta(\pi/2)/t = \alpha m_p/t$. After the drop, the dimerization gap and the phonon order parameter decrease as the phonon frequency increases. At the critical value ω_c, the dimerization gap and the phonon order parameter go to zero simultaneously, and the system becomes gapless, which indicates that the quantum lattice fluctuations can destroy the dimerized Peierls state. The dimerization gap is much more reduced by the quantum lattice fluctuations than the phonon order parameter. The reason for the different behavior of the dimerization gap and the order parameter is that the former is the value of Eq. (14) at the Fermi point $k = \pi/2$, where the quantum lattice fluctuations have the strongest effect, while the latter is the integral [see Eq. (12)] over the all Brillouin zone, and the effect of the quantum lattice fluctuations is calmed. The effects of quantum lattice fluctuations on the dimerization gap and on the phonon order parameter are essentially different, especially when ω_0 is small. In the mean field (MF) approximation, the Peierls distortion opens a gap of $2\Delta_{MF}$ and $\Delta_{MF} = \alpha m_p$. That relation is sometimes assumed remains valid when quantum lattice fluctuations are taken into account. Our results indicate that this relation holds only in the adiabatic limit.

The optical conductivity $\sigma(\omega)$ can be expressed by the retarded Green's function as follows:

$$\sigma(\omega) = -\frac{2\varepsilon_0 nc}{\pi\omega} \text{Im} K^R(\omega), \qquad (15)$$

where K^R is defined as

$$K^R(\omega) = -i \int_{-\infty}^{0} e^{-i\omega t} dt \langle g|[j(0)j(t) - j(t)j(0)]|g\rangle. \qquad (16)$$

Here, j is the current operator,[16]

TABLE I. Critical point g_c. g^* is the value of g determined by letting the stiffness constant $K_\rho = \frac{1}{2}$.

t/ω_0	0.05	0.1	0.5	1	5	10	20	100
g_c/ω_0 (Ref. 12)	2.297(2)	2.093(2)	1.63(1)	1.61(1)	2.21(3)	2.79(5)		
g^*/ω_0 (Ref. 12)	2.299	2.102	1.64	1.62	2.27	2.89		
g_c/ω_0	2.8215	2.1613	1.5939	1.6403	2.3068	2.8783	3.6868	6.9738

$$j = -ieta \sum_l (c_l^\dagger c_{l+1} - c_{l+1}^\dagger c_l), \qquad (17)$$

and $j(t) = \exp(iHt) j \exp(-iHt)$ is the form of j in the Heisenberg representation. The unitary transformation of the current operator is $e^S j e^{-S} = j + [S,j] + \frac{1}{2}[S,[S,j]] + O(g^3)$. All terms of order higher than g^2 will be omitted in the following treatment. Because the averaging of $\tilde{H}_1$ over the phonon vacuum state is zero, in the ground state at zero temperature $\tilde{H}_1$ can be neglected. By using the approximately decoupling $|g'\rangle \approx |g_0'\rangle$, the ground state of $\tilde{H}_0$, and $\tilde{H} \approx \tilde{H}_0$ in the calculation

$$
\begin{aligned}
\langle g|j(0)j(t)|g\rangle &= \langle g'|[e^{(S+R)} j e^{-(S+R)}] e^{i\tilde{H}t} \\
&\quad \times [e^{(S+R)} j e^{-(S+R)}] e^{-i\tilde{H}t}|g'\rangle \\
&\approx \langle g_0'|[e^S j e^{-S}] e^{i\tilde{H}_0 t} [e^S j e^{-S}] e^{-i\tilde{H}_0 t}|g_0'\rangle,
\end{aligned}
\qquad (18)
$$

we can get

$$
\begin{aligned}
K^R(\omega) &= \frac{J^2}{N} \sum_{k>0} \left(\frac{1}{\omega - 2W_k + i0^+} - \frac{1}{\omega + 2W_k - i0^+} \right) \sin^2 k \\
&\quad \times \left[1 - \frac{2}{N} \sum_{k'} \frac{g^2}{\omega_0^2} \delta^2(k',k) \right] \frac{\Delta_k^2}{W_k^2} \\
&\quad + \frac{J^2}{N^2} \sum_{k>0,k'>0} \frac{g^2}{\omega_0^2} \left(\frac{1}{\omega - \omega_0 - W_k - W_{k'} + i0^+} \right. \\
&\quad \left. - \frac{1}{\omega + \omega_0 + W_k + W_{k'} - i0^+} \right) [\delta^2(k',k) \\
&\quad \times (\sin k' - \sin k)^2 (\alpha_k \beta_{k'} + \beta_k \alpha_{k'})^2 + \delta^2(k' - \pi, k) \\
&\quad \times (\sin k' + \sin k)^2 (\alpha_k \alpha_{k'} + \beta_k \beta_{k'})^2],
\end{aligned}
\qquad (19)
$$

where $\alpha_k = \sqrt{(1 + E_k/W_k)/2}$, and $\beta_k = \sqrt{(1 - E_k/W_k)/2}$. Thus, we have the optical conductivity

$$
\begin{aligned}
\sigma(\omega) &= \frac{2\varepsilon_0 nc J^2}{\omega} \sum_{k>0} \delta(\omega - 2W_k) \sin^2 k \\
&\quad \times \left[1 - \frac{2}{N} \sum_{k'} \frac{g^2}{\omega_0^2} \delta^2(k',k) \right] \frac{\Delta_k^2}{W_k^2} \\
&\quad + \frac{2\varepsilon_0 nc J^2}{\omega N} \sum_{k>0,k'>0} \frac{g^2}{\omega_0^2} \delta(\omega - \omega_0 - W_k - W_{k'}) \\
&\quad \times [\delta^2(k',k)(\sin k' - \sin k)^2 (\alpha_k \beta_{k'} + \beta_k \alpha_{k'})^2 \\
&\quad + \delta^2(k' - \pi, k)(\sin k' + \sin k)^2 (\alpha_k \alpha_{k'} + \beta_k \beta_{k'})^2],
\end{aligned}
\qquad (20)
$$

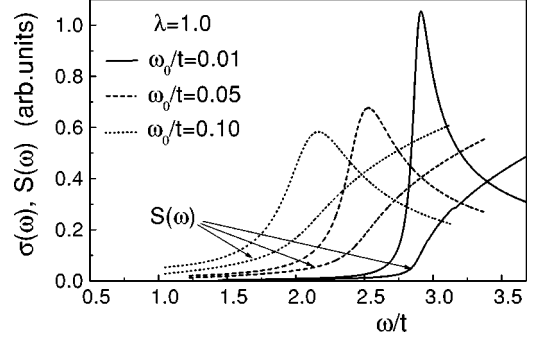and the ω-integrated spectral-weight function

FIG. 3. The optical conductivity in the case of $\lambda = 1.0$ for different phonon frequencies $\omega_0/t = 0.01$, 0.05, and 0.10.

$$S(\omega) = \int_0^\omega \sigma(\omega') d\omega'. \qquad (21)$$

The optical conductivity for different phonon frequencies are shown in Fig. 3. The parameter values used are $\lambda = 1.0$, with $\omega_0/t = 0.01$, 0.05, and 0.10. One can see that as ω_0 increases, the optical-absorption spectrum broadens but the peak height decreases and moves to lower photon energy, and the spectral weight increases as ω_0 increases. The inverse-square-root singularity at the gap edge in the adiabatic case[17] disappears and there is a significant tail below the peak because of the nonadiabatic effect. We note that in our theory, in mathematical viewpoint, the difference between the $\omega_0 = 0$ and $\omega_0 > 0$ cases mainly comes from the functional form of the gap [see Eq. (8)]. Comparing it with that in the adiabatic limit, one can see that the subgap states come from the quantum lattice fluctuations, i.e., the second term in the square bracket of Eq. (8).

The rescaled ω-integrated spectral-weight function $S(\omega)/S_m$ versus the photon energy ω/t relations of our result (solid line) and that of IMVLF (dashed line) are shown in Fig. 4, where $S_m = S(\omega \to \infty)$. The optical conductivity $\sigma(\omega)$ (rescaled by S_m) of our result (solid line) is also shown.
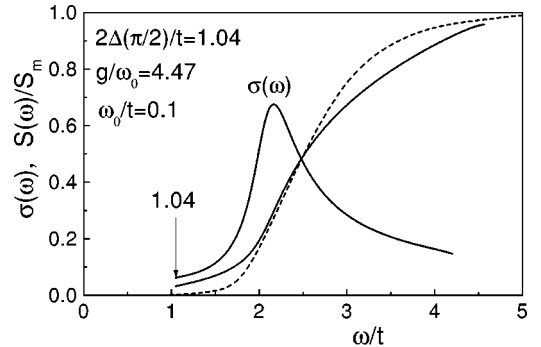

FIG. 4. The rescaled optical conductivity $\sigma(\omega)$ and ω-integrated spectral-weight function $S(\omega)/S_m$ versus the photon energy ω/t relations of our results and that of IMVLF, where $S_m = S(\omega \to \infty)$. The parameter values used are the same as in Ref. 14, Fig. 6(b): $g/\omega_0 = 4.47$ and $\omega_0/t = 0.1$. The dashed line is the result of IMVLF, and the solid lines are our results. The arrow marks the true gap $2\Delta(\pi/2)/t = 1.04$.

Because of the finite-size effects, the optical conductivity of IMVLF is oscillatory and can not be compared with our result directly. We use the same parameter values as in Ref. 13, Fig. 6(b): $g/\omega_0=4.47$ and $\omega_0/t=0.1$. The true gap $2\Delta(\pi/2)/t=1.04$ obtained from Eq. (14) is marked by the arrow. One can see that the peak of optical-conductivity spectrum is not directly corresponding to the dimerized gap. The energy gap is smaller than the activation energy of the optical conductivity. Our result shows clearly both the position and the peak of optical conductivity and the spectral weight agrees with that of IMVLF, while in the exact-diagonalization method, the finite-size effects prevent a precise extraction of the CDW gap from the optical exact-diagonalization data.[13]

In conclusion, the effects of quantum lattice fluctuations on the optical-conductivity spectrum and the ground-state phase diagram of the one-dimensional Holstein model of spinless fermions have been studied by developing an analytical approach. We show that when the electron-phonon coupling constant decreases, the dimerization gap decreases, and at a finite critical value, the Peierls dimerization is destroyed by the quantum lattice fluctuations. The critical value of electron-phonon coupling can be determined precisely even for very small phonon frequency. The dimerization gap is much more reduced by the quantum lattice fluctuations than the order parameter. The calculated optical conductivity does not have the inverse-square-root singularity but it has a peak above the gap edge, and there exists a significant tail below the peak. In the nonadiabatic case, the dimerization gap is smaller than what the peak position of the optical conductivity is corresponding to. Our results of the phase diagram and the spectral-weight function agree with those of the density-matrix renormalization group and the exact-diagonalization methods.

*Email address: hzheng@online.sh.cn

[1] T. Holstein, Ann. Phys. (N.Y.) **8**, 325 (1959).

[2] R.H. McKenzie and J.W. Wilkins, Phys. Rev. Lett. **69**, 1085 (1992); K. Kim, R.H. McKenzie, and J.W. Wilkins, *ibid.* **71**, 4015 (1993).

[3] E. Fradkin and J.E. Hirsch, Phys. Rev. B **27**, 1680 (1983).

[4] T.W. Hagler and A.J. Heeger, Phys. Rev. B **49**, 7313 (1994).

[5] H. Zheng, Phys. Rev. B **56**, 14 414 (1997).

[6] J.E. Hirsch and E. Fradkin, Phys. Rev. B **27**, 4302 (1983).

[7] R.H. McKenzie, C.J. Hamer, and D.W. Murray, Phys. Rev. B **53**, 9676 (1996).

[8] C. Bourbonnais and L.G. Caron, J. Phys. (Paris) **50**, 2751 (1989).

[9] D. Schmeltzer, J. Phys. C **18**, L1103 (1985).

[10] H. Zheng, D. Feinberg, and M. Avignon, Phys. Rev. B **39**, 9405 (1989).

[11] G. Wellein and H. Fehske, Phys. Rev. B **56**, 4513 (1997).

[12] R.J. Bursill, R.H. McKenzie, and C.J. Hamer, Phys. Rev. Lett. **80**, 5607 (1998).

[13] A. Weisse and H. Fehske, Phys. Rev. B **58**, 13 526 (1998).

[14] H. Zheng and M. Avignon, Phys. Rev. B **58**, 3704 (1998).

[15] L.G. Caron and C. Bourbonnais, Phys. Rev. B **29**, 4230 (1984).

[16] C. Zhang, E. Jeckelmann, and R. White, Phys. Rev. B **60**, 14 092 (1999).

[17] J.T. Gammel, I. Batistic, A.R. Bishop, E.Y. Loh, Jr., and S. Marianer Physica B **163**, 458 (1990).